Accepted for publication in Journal of Low Temperature Physics.

Multi-pair and exchange effects in the dynamic structure of two–dimensional ^{3}He

R. Hobbiger[†], R. Holler[†], E. Krotscheck[†+] and M. Panholzer[†]

[†]*Institut für Theoretische Physik, Johannes Kepler Universität, A 4040 Linz, Austria*

[+]*Department of Physics, University at Buffalo SUNY, Buffalo, NY 14260*

Abstract

We examine the effect of fermionic exchange interactions on the dynamic structure function of two-dimensional ^{3}He within a manifestly microscopic theory of excitations. These exchanges have, at different wave lengths and densities, different consequences: At low densities, exchanges are decisive to determine whether the phonon is Landau-dampened or not. In the intermediate wave number regime, exchanges are relatively unimportant but they become important again at short wave length corresponding to about four times the Fermi wave number.

A very important further aspect is the inclusion of pair fluctuations. These are fluctuations of the wave function that can not be described by the quantum numbers of a single particle. They do not change the features of long wave length excitations, but induce a finite width to the collective mode outside the particle-hole continuum. In the intermediate momentum regime, where one would expect a "roton minimum" in a Bose fluid with the same interaction and density, pair fluctuations cause a visible shift of the strength of the dynamic structure function towards lower energies and cause a very sharp collective mode. The effect, which was reported by Godfrin *et al.*, Nature **483**, 576 (1012), is slightly enhanced by exchange corrections.

PACS numbers: 67.30.-n, 67.30.em

I. INTRODUCTION

The helium fluids are the prime example of both bosonic (^{4}He) and fermionic (^{3}He) strongly correlated quantum many-body systems. Governed by a simple Hamiltonian, yet very dense, they have been studied for decades and still offer surprises leading to new insights. A new development in our understanding of liquid ^{3}He is the unexpected appearance of a collective excitation at short wave lengths in quasi-two-dimensional ^{3}He[1]. This mode was discovered experimentally by neutron scattering experiments, and independently predicted by a microscopic dynamic many-body calculation.

The main quantity describing the dynamics of the system is its dynamic structure function $S(q;\omega)$, which is closely related to the response of the system to a weak, time-dependent perturbation. Experimentally, the dynamic structure function of ^{3}He is mostly determined by neutron- or X-ray scattering, the theoretical and experimental understanding a decade ago has been summarized in Ref. 2.

We report here microscopic calculations for the structure and the dynamics of two-dimensional ^{3}He. In particular, we examine the importance of exchange interactions. The next section gives a very brief compilation of our techniques. We deliberately refrain from any explanation and refer to the original work and earlier review- and pedagogical material[3,4] for details. The basis of our dynamic theory[5] is the generalization of the work of Jackson, Feenberg, and Campbell[6–8], who included pair-fluctuations in the dynamic wave function of a Bose fluid, to Fermions. We have in Ref. 5 formulated a strategy for including such pair-excitation effects in Fermi fluids. In our recent work[1] and in a related analysis[9] of X-ray experiments on ^{3}He, we have used the simplest implementation of that theory. Two potentially significant corrections have not been included in that work: dynamic self–energy corrections and exchange effects.

Dynamic self–energy corrections play mostly a role at low energies. Due to spin fluctuations, the effective mass around the Fermi momentum is strongly enhanced[10], our theoretical calculations are in good agreement with experiments[11–13]. The effect dies out rapidly as a function of energy, it should therefore be of minor importance for the results to be reported here. Self-energy corrections should, of course, have important consequences for the spin-structure function.

The second important effect is fermionic exchange. The implementation of our dynamic

many-body theory used in Ref. 1 deals with exchanges in a local approximation whose quality is hard to assess from a general point of view. Thus, the purpose of this paper is a theoretical study of the importance of exchange processes which were not included in our previous work.

II. DYNAMIC MANY-BODY THEORY

A. Ground State Many-Body Theory

We base our calculations on the variational Jastrow-Feenberg theory, including corrections from correlated basis functions (CBF) theory. The application of the theory to ^{3}He has been described in Ref. 3, we have implemented exactly the same approach in two dimensions.

Microscopic many-body theory starts from a phenomenological Hamiltonian for N interacting particles,

$$H = -\sum_i \frac{\hbar^2}{2m}\nabla_i^2 + \sum_{i<j} v\left(|\mathbf{r}_i - \mathbf{r}_j|\right) . \tag{1}$$

For strong interactions, CBF theory[7] has proven to be an efficient and accurate method to obtain ground-state properties. It starts with a variational wave function of the form

$$|\Psi_o\rangle = \frac{F\,|\Phi_o\rangle}{\langle\Phi_o|\,F^\dagger F\,|\Phi_o\rangle^{1/2}} , \tag{2}$$

where $\Phi_o(1,\ldots,i,\ldots,N)$ is a model state, normally a Slater–determinant, and "i" is short for both spatial and discrete (spin and/or isospin) degrees of freedom. The *correlation operator* $F(1,\ldots,N)$ is suitably chosen to describe the important features of the interacting system. Most practical and successful is the Jastrow–Feenberg[7] form

$$F(1,\ldots,N) = \exp\left\{\frac{1}{2}\left[\sum_{1\le i<j\le N} u_2(\mathbf{r}_i,\mathbf{r}_j) + \sum_{1\le i<j<k\le N} u_3(\mathbf{r}_i,\mathbf{r}_j,\mathbf{r}_k) + \ldots\right]\right\} . \tag{3}$$

The *correlation functions* $u_n(\mathbf{r}_1,\ldots,\mathbf{r}_n)$ are ensured to be unique by imposing the "cluster property", $u_n(\mathbf{r}_1,\ldots,\mathbf{r}_n) \to 0$ if $|\mathbf{r}_i - \mathbf{r}_j| \to \infty$, for any pair of coordinates $\mathbf{r}_i$, $\mathbf{r}_j$.

From the wave function (2), (3), the energy expectation value

$$H_{o,o} \equiv \langle\Psi_o|\,H\,|\Psi_o\rangle \tag{4}$$

can be calculated either by simulation or by integral equation methods. The hierarchy of Fermi-Hypernetted-Chain (FHNC) approximations is compatible with the optimization

problem, *i.e.* with determining the optimal *correlation functions* $u_n(\mathbf{r}_1, \ldots, \mathbf{r}_n)$ through functionally minimizing the energy

$$\frac{\delta H_{\text{o,o}}}{\delta u_n(\mathbf{r}_1, \ldots, \mathbf{r}_n)} = 0\,. \tag{5}$$

The results of diagrammatic many-body calculations provide necessary input for the analysis of the dynamics to be described below, most of them cannot be obtained from Monte Carlo calculations. It is, of course, an important verification of our theory that those quantities, that can be obtained from Monte Carlo calculations, are reproduced with acceptable accuracy. We show in Fig. 1 a comparison of the FHNC-EL and Monte Carlo[14,15] results for the energy, together with a breakdown into the contributions from the optimized Fermi-Hypernetted-Chain (FHNC-EL) theory, triplet correlations, elementary diagrams, and CBF corrections. The relative size of the individual corrections is comparable to those in both two-dimensional ^{4}He as well as in ^{3}He in three dimensions; CBF corrections are negligible except at very high densities. Considering the rather crude evaluation of elementary diagrams, the agreement between FHNC-EL and MC results is actually quite satisfactory. Note in particular that the total energy comes from a rather significant cancellation between kinetic and potential energy which enhances small errors.

A similar observation applies to the static structure functions. Fig. 2 compares the simplest FHNC-EL version, the version containing elementary diagrams and triplet correlations, and simulation data[16], for two representative densities. In general, the agreement is good for all practical purposes, in particular the results from the simplest FHNC-EL version match the Monte Carlo data quite well.

Two observations are made at high density:

- The peak in $S(k)$ predicted by the FHNC version with triplet correlations and elementary diagrams is visibly higher that the one obtained from Monte Carlo calculations. At this point, we are not ready to attribute a higher reliability to one calculation over the other. The peak in $S(k)$ is related to long-ranged oscillations in the pair distribution function, caused by the impeding liquid-solid phase transition. To get this peak right, one must have the pair distribution function at rather large distances; the FHNC calculation has been carried out in a box of 280 Å. Replacing $g(r)$ for $r > 10$ Å with its asymptotic value of 1 and calculating the Fourier transform, this peak is much lowered.

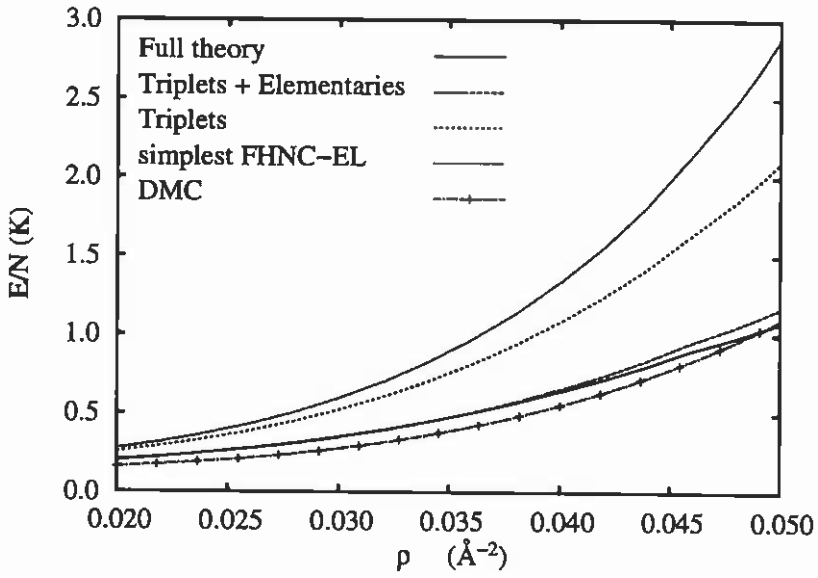

FIG. 1. The figure shows the breakdown of the equation of state of two-dimensional ^{3}He into contributions from the simplest FHNC-EL theory, triplet correlations, elementary diagrams and CBF corrections. The line with markers shows the fit to the equation of state of 2D ^{3}He obtained from Monte Carlo calculations[14,15].

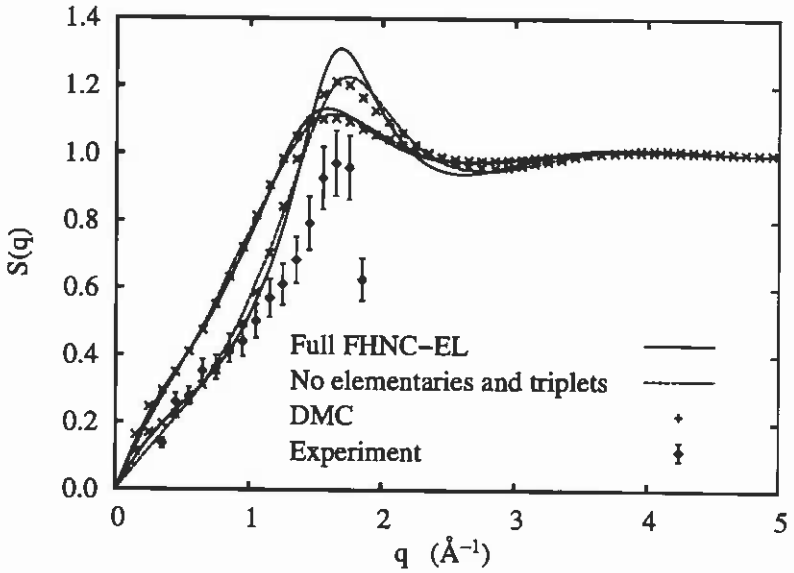

FIG. 2. The figure shows the structure function $S(q)$ for 2D ^{3}He in FHNC-EL (long-dashed lines), including triplet correlations and elementary diagrams (solid lines), and from Monte Carlo calculations (crosses)[16] for the two representative densities $\rho = 0.032\,\text{Å}^{-2}$ and $\rho = 0.046\,\text{Å}^{-2}$. The curves with the higher peak correspond to the higher density. The diamonds with error bars have been obtained[17] by integrating the experimental data of Ref. 1.

- A small "shoulder" of $S(k)$ is observed for $k < 0.3\,\text{Å}^{-1}$, which reflects the fact that $S(k) \leq \hbar k/2mc$ for small k, where c is the speed of sound. Since the inclusion of elementary diagrams and triplet correlations adds binding to the system, the speed of sound becomes smaller, the slope steeper, and the agreement becomes better.

The figure also shows some experimental data that were obtained by calculating[17] the energy integral (16) of the experimental data published in Ref. 1. They fall short of the theoretical value at larger momentum transfers most likely due to a too low energy cutoff.

Given the uncertainty in the peak value of $S(k)$ at high densities, we have used the results from the simplest FHNC-EL version as input to our calculations of the dynamics.

B. Equations of Motion

The dynamics of the system is treated with the logical generalization of the wave function (2), (3) to dynamic correlations by writing the response of the system to a weak and time dependent external field $H_{\text{ext}}(t) = \sum_i \delta h_{\text{ext}}(\mathbf{r}_i; t)$ in the form

$$\begin{aligned} |\Psi(t)\rangle &= \frac{1}{\sqrt{\mathcal{N}}}\, e^{-\mathrm{i}E_0 t/\hbar}\, |\Psi_0(t)\rangle \ , \\ |\Psi_0(t)\rangle &= F\, e^{\frac{1}{2}\delta U(t)}\, |\Phi_0\rangle \quad , \quad \mathcal{N} \equiv \langle \Psi_0(t)\,|\,\Psi_0(t)\rangle \ . \end{aligned} \tag{6}$$

where F is taken from the ground state calculation, and $\delta U(t)$ is a sum of n–particle–n–hole excitation operators:

$$\delta U(t) = \sum_{ph} \delta u^{(1)}_{ph}(t)\, a^\dagger_p a_h + \tfrac{1}{2} \sum_{pp'hh'} \delta u^{(2)}_{pp'hh'}(t)\, a^\dagger_p a^\dagger_{p'} a_{h'} a_h + \ldots \ . \tag{7}$$

As a convention, we will label "particle" (unoccupied) and "hole" (occupied) states with p, p' and h, h', respectively. Discrete (*e.g.* spin) degrees of freedom are suppressed.

Equations of motion for the $\delta u^{(i)}(t)$ are derived from the action principle[18,19]

$$\delta \int dt \left\langle \Psi(t) \left| H + H_{\text{ext}}(t) - \mathrm{i}\hbar \frac{\partial}{\partial t} \right| \Psi(t) \right\rangle = 0 \, . \tag{8}$$

To obtain a density-density response function, the equations of motion are linearized. The analytic and diagrammatic manipulations to bring the resulting equations of motion into a numerically tractable form are lengthy and delicate[5], but the result is surprisingly simple and can be cast into the familiar form of the time-dependent Hartree-Fock (TDHF) theory[20]

with *energy-dependent* effective interactions. The induced density fluctuations are expanded in terms of matrix elements of the density operator in the non-interacting system, $\rho^F_{0,ph}(\mathbf{r}) = \langle h|\delta\hat{\rho}(\mathbf{r})|p\rangle$.

$$\delta\rho(\mathbf{r};\omega) = \frac{1}{2}\sum_{ph}\left[\rho^{\rm F}_{0,ph}(\mathbf{r})\,\delta c^{(+)}_{ph}(\omega) + \rho^{\rm F*}_{0,ph}(\mathbf{r})\,\delta c^{(-)}_{ph}(\omega)\right]\,. \tag{9}$$

The amplitudes $\delta c^{(\pm)}_{ph}(\omega)$ are related by the THDF equations to the matrix elements $h_{ij} = \langle i|\delta h_{\rm ext}|j\rangle$ of the external field,

$$\begin{pmatrix} V^{(A)}_{ph,p'h'}(\omega) + (\hbar\omega - e_{ph})\delta_{ph,p'h'} & V^{(B)}_{pp'hh',0}(\omega) \\ V^{(B)}_{0,pp'hh'}(\omega) & V^{(A)}_{p'h',ph}(\omega) - (\hbar\omega + e_{ph})\delta_{ph,p'h'} \end{pmatrix} \begin{pmatrix} \delta c^{(+)}_{p'h'} \\ \delta c^{(-)}_{h'p'} \end{pmatrix} = 2\begin{pmatrix} h_{ph} \\ h_{hp} \end{pmatrix}\,, \tag{10}$$

where $\delta_{ph,p'h'} = \delta_{p,p'}\delta_{h,h'}$ and $e_{ph} = e(p) - e(h)$ is the particle-hole excitation energy of the correlated system,

$$e(q) = t(q) + V_1(q)\,. \tag{11}$$

$t(q) = \hbar^2q^2/2m$ is the kinetic energy of a free particle, and $V_1(q)$ the correlation correction[21].

Supressing arguments in the potentials, the response function is

$$\chi(q;\omega) = \begin{pmatrix} \rho^{\rm F}_{0,ph} \\ \rho^{\rm F*}_{0,ph} \end{pmatrix}^{\dagger} \begin{pmatrix} V^{(A)}_{ph,p'h'} + (\hbar\omega - e_{ph})\delta_{ph,p'h'} & V^{(B)}_{pp'hh',0} \\ V^{(B)}_{0,pp'hh'} & V^{(A)}_{p'h',ph} - (\hbar\omega + e_{ph})\delta_{ph,p'h'} \end{pmatrix}^{-1} \begin{pmatrix} \rho^{\rm F}_{0,p'h'} \\ \rho^{\rm F*}_{0,p'h'} \end{pmatrix}\,. \tag{12}$$

In essence, the machinery of microscopic many-body theory leads to a definition of the effective interactions $V^{(A)}_{ph,p'h'}(\omega)$ and $V^{(B)}_{pp',hh'}(\omega)$ appearing in the well-known TDHF equations in terms of the correlation operator F and the underlying microscopic Hamiltonian.

C. Effective interactions

The simplest approximation one can make for the matrix elements $V^{(A)}_{ph,p'h'}(\omega)$ and $V^{(B)}_{pp'hh',0}(\omega)$ is that they are local,

$$V^{(A,B)}_{ph,p'h'}(\omega) = \frac{\delta_{\mathbf{p+h},\pm(\mathbf{p'-h'})}}{N}\,\tilde{V}^{(A,B)}(q;\omega)\,. \tag{13}$$

If, furthermore, the effective interactions are assumed *energy independent* and equal in A and B channel, *i.e.* $\tilde{V}^{(A)}(q;\omega) = \tilde{V}^{(B)}(q;\omega) \equiv \tilde{V}_{\rm p-h}(q)$, the theory collapses to the familiar RPA form of linear response theory

$$\chi(q;\omega) = \frac{\chi_0(q;\omega)}{1 - \widetilde{V}_{\rm p\text{-}h}(q)\,\chi_0(q;\omega)}\,. \tag{14}$$

Here, $\chi_0(q;\omega)$ is the Lindhard function, and $\tilde{V}_{\text{p-h}}(q)$ is known as the "particle–hole interaction" or "pseudo–potential[22]". $\chi(q;\omega)$ is related to the dynamic structure function

$$S(q;\omega) = -\frac{\hbar}{\pi}\Im m[\chi(q;\omega)]\,\theta(\omega) \tag{15}$$

which satisfies, amongst others, the sum rules

$$m_0(q) = S(q) = \int_0^\infty d(\hbar\omega)\; S(q;\omega), \tag{16}$$

$$m_1(q) = \frac{\hbar^2 q^2}{2m} = \int_0^\infty d(\hbar\omega)\; \hbar\omega\, S(q;\omega)\,, \tag{17}$$

where $S(q)$ is the static structure factor. In the RPA, the sum rules (16) and (17) can be used to define a local particle-hole interaction $\tilde{V}_{\text{p-h}}(q)$.

The RPA (14) for $\chi(q;\omega)$ displays the essential features of the dynamic structure function $S(q;\omega)$ qualitatively correctly: $S(q;\omega)$ can be characterized as being a superposition of a collective mode similar to the phonon-maxon-roton in ^{4}He, *plus* an incoherent particle-hole band which strongly dampens this mode where it is kinematically allowed. However, the RPA as defined here predicts a zero-sound mode that is significantly too high. This is consistent with the same deficiency of the Feynman spectrum $\varepsilon(q) = \hbar^2 q^2/2mS(q)$ in ^{4}He.

Our dynamic many-body theory cures this deficiency to a large extent by including pair-fluctuations $u^{(2)}_{pp'hh'}(t)$ in the excitation operator. Among others, this introduces a frequency dependence. In Ref. 5 we have derived working formulas for the effective interactions in terms of a three-body vertex and a pair propagator, which are generalizations of the bosonic version[6–8]. The components of the energy-dependent interactions $V_{\text{A,B}}(q;\omega)$ are

$$\tilde{V}^{(A)}(q;\omega) = \tilde{V}_{\text{p-h}}(q) + [\sigma_q^+]^2\,\widetilde{W}(q;\omega) + [\sigma_q^-]^2\,\widetilde{W}^*(q;-\omega) \tag{18}$$

$$\tilde{V}^{(B)}(q;\omega) = \tilde{V}_{\text{p-h}}(q) + \sigma_q^+\sigma_q^-\,\left[\widetilde{W}(q;\omega) + \widetilde{W}^*(q;-\omega)\right]\,, \tag{19}$$

with $\sigma_q^\pm \equiv [S_{\text{F}}(q) \pm S(q)]/2S(q)$. Here, $\tilde{V}_{\text{p-h}}(q)$ is the static part of the particle-hole interaction that is related to the static structure function through the RPA relationship (14) and the two sum rules (16) and (17).

The energy dependent part of the interaction $\widetilde{W}(q;\omega)$ describes the splitting and recombination of phonons; it consists of a three-phonon vertex $\tilde{K}_{q,q'q''}$ and a two-phonon propagator $\tilde{E}^{-1}(q',q'';\omega)$:

$$\widetilde{W}(q;\omega) = \frac{1}{2N}\sum_{\mathbf{q}',\mathbf{q}''}\delta_{\mathbf{q}+\mathbf{q}'+\mathbf{q}''}|\tilde{K}_{q,q'q''}|^2\,\tilde{E}^{-1}(q',q'';\omega) \tag{20}$$

with the three-body vertex

$$\bar{K}_{q,q'q''} = \frac{\hbar^2}{2m} \frac{S(q')S(q'')}{S_{\rm F}(q)S_{\rm F}(q')S_{\rm F}(q'')} \left[\mathbf{q}\cdot\mathbf{q}'\, \tilde{X}_{\rm dd}(q') + \mathbf{q}\cdot\mathbf{q}''\, \tilde{X}_{\rm dd}(q'') - q^2 \tilde{u}_3(q,q',q'') \right] . \qquad (21)$$

Here, $S_{\rm F}(q)$ is the static structure function of non-interacting fermions, $\tilde{X}_{\rm dd}(q)$ is the set of "non-nodal" diagrams of the Fermi-hypernetted-chain theory, and $u_3(q,q',q'')$ is the three-body ground state correlation[3].

The pair propagator is

$$\bar{E}^{-1}(q_1,q_2;\omega) = -\int_{-\infty}^{\infty} \frac{d(\hbar\omega')}{2\pi \mathrm{i}}\, \kappa(q_1;\omega')\, \kappa(q_2;\omega-\omega') \qquad (22)$$

$$\kappa(q;\omega) = \frac{\kappa_0(q;\omega)}{1+\hbar\omega\tilde{\Gamma}_{\rm dd}(q)\kappa_0(q;\omega)} \qquad (23)$$

with the "direct-direct" correlation function $\bar{\Gamma}_{\rm dd}(q)$, and the partial Lindhard function:

$$\kappa_0(q;\omega) \equiv \frac{1}{N}\sum_h \frac{\bar{n}_{\rm p} n_{\rm h}}{\hbar\omega - e_{ph} + \mathrm{i}\eta} . \qquad (24)$$

For the execution of this version of the theory at that level we need only the static structure function $S(q)$. This is because the energy independent part of the particle-hole interaction $\widetilde{V}_{\text{p-h}}(q)$ can still be obtained from the sum rules (16) and (17): the dynamic correction $\widetilde{W}(q;\omega)$ causes negligible change to these sum rules[5]. In fact, for bosons it has been proven[23] that the dynamic corrections do not change the outcome of the energy integration at all.

It is clear, however, that the local approximations imply a rather crude treatment of fermionic exchange. More general effective interactions are also readily derived from CBF theory[21,24]. Keeping exchanges explicitly, the matrix elements appearing in the TDHF equation are of the structure

$$\begin{aligned} V^{(A)}_{ph,p'h'}(\omega) &= \langle ph' | V^{(A)}_{\rm dd}(1,2) | hp' \rangle - \langle ph' | V^{(A)}_{\rm ex}(1,2) | p'h \rangle , \\ V^{(B)}_{pp'hh',0}(\omega) &= \langle pp' | V^{(B)}_{\rm dd}(1,2) | hh' \rangle - \langle pp' | V^{(B)}_{\rm ex}(1,2) | h'h \rangle . \end{aligned} \qquad (25)$$

The static, energy independent parts of all four of these operators have been evaluated in terms of the diagrammatic elements of CBF theory[21,24], they are in principle also non-local but dominated by their local term which depends only on the distance between the particles. These local terms are natural byproducts of an FHNC-EL calculation, specifically $\widetilde{V}_{\text{p-h}}(q)$, $\tilde{V}_{\rm dd}(q)$ and $\tilde{V}_{\rm ex}(q)$ as defined in Ref. 3, Eqs. (2.25) and (3.25). These interactions are *not*

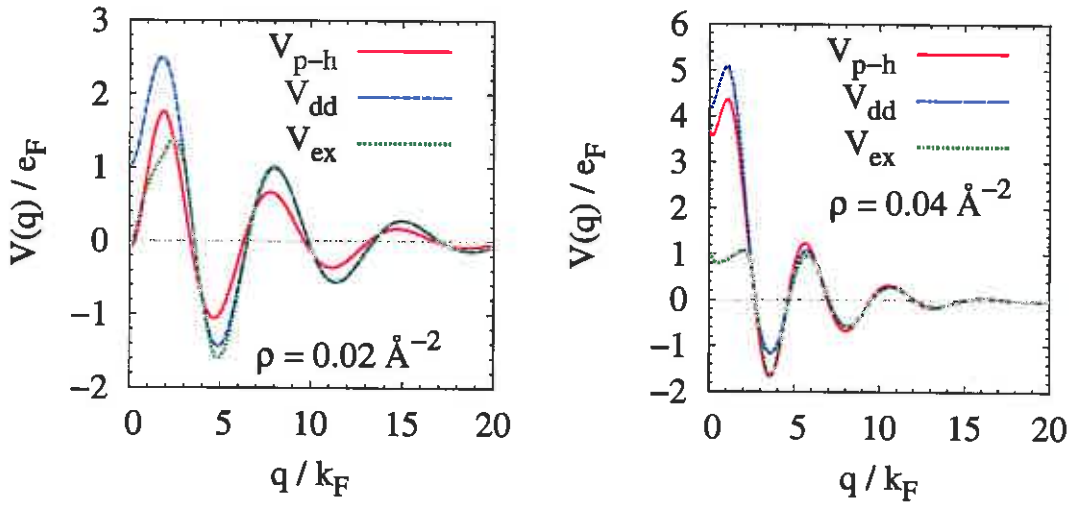

FIG. 3. The figure shows the local pseudopotential $\tilde{V}_{\text{p-h}}(q)$ (solid line), the direct channel interaction $V_{\text{dd}}(q)$ (dashed-dotted line) and the exchange-channel interaction $V_{\text{ex}}(q)$ (short-dashed line) for the two different densities $\rho = 0.02\,\text{Å}^{-2}$ (left pane) and $\rho = 0.04\,\text{Å}^{-2}$ (right pane).

the same, $\tilde{V}_{\text{dd}}(q)$ does not contain nodal diagrams whereas $\tilde{V}_{\text{ex}}(q)$ does. Also, the direct term $\tilde{V}_{\text{dd}}(q)$ can no longer be obtained through the sum rules (16) and (17) because exchange terms contribute to the static stricture function. $\tilde{V}_{\text{dd}}(q)$ is therefore also *different* from the $\tilde{V}_{\text{p-h}}(q)$ introduced above. The two different interactions are shown, for the densities $\rho = 0.02\,\text{Å}^{-2}$ and $\rho = 0.04\,\text{Å}^{-2}$ in Figs. 3, for completeness we also show the exchange-channel potential $\tilde{V}_{\text{ex}}(q)$. Evidently the three functions are rather similar and basically differ only in their long–wavelength part. This is not surprising since they describe basically the same physics (see Ref. 22: core exclusion, a slight swelling of the core due to the kinetic energy that comes from bending the wave function, and long-ranged correlation's manifested in the long-wavelength limit. All the short-ranged features, which appear in momentum space as oscillations ranging out to large momenta, of the three effective potentials are the same, the three potentials differ only in their long-wavelength parts. In particular, long-ranged correlations appear to be less important at low densities, therefore $\tilde{V}_{\text{dd}}(q)$ and $\tilde{V}_{\text{ex}}(q)$ are practically the same at $\rho = 0.02\,\text{Å}^{-2}$. In an exact theory, $\tilde{V}_{\text{p-h}}(0+) \approx m(c^2 - c_F^2)$ where c is the speed of sound, and c_F is the Fermi velocity. Note that $\tilde{V}_{\text{p-h}}(0+) < 0$ at the small density which is a signature that the sound mode is Landau dampened.

In this work, we supplement the direct term with the energy-dependent phonon-splitting

corrections spelled out in Eqs. (18) and (19), *i.e.* we have

$$\tilde{V}_{\rm dd}^{(A)}(q;\omega) = \tilde{V}_{\rm dd}(q) + [\sigma_q^+]^2\,\widetilde{W}(q;\omega) + [\sigma_q^-]^2\,\widetilde{W}^*(q;-\omega) \tag{26}$$

$$\tilde{V}_{\rm dd}^{(B)}(q;\omega) = \tilde{V}_{\rm dd}(q) + \sigma_q^+\sigma_q^-\,\left[\widetilde{W}(q;\omega) + \widetilde{W}^*(q;-\omega)\right]\,. \tag{27}$$

When we include exchange contributions, to be consistent[25] the single-particle energies e_{ph} must contain correlation corrections which are just the Fock terms of the exchange potential $\tilde{V}_{\rm ex}(q)$,

$$V_{\rm i}(q) = -\sum_h \langle qh|V_{\rm ex}|hq\rangle\,. \tag{28}$$

III. DYNAMIC STRUCTURE OF TWO-DIMENSIONAL ^{3}HE

We have carried out a comprehensive array of calculations of $S(q;\omega)$ for two-dimensional ^{3}He in the density regime between densities of $\rho = 0.02\,\text{Å}^{-2}$ and $\rho = 0.05\,\text{Å}^{-2}$ and wave numbers up to $q = 4\,k_F$ ($k_F = \sqrt{2\pi\rho}$ is the Fermi momentum).

We have carried out four levels of calculations:

- ("RPA") A simple RPA calculation that omits exchange effects and determines the direct interaction $\widetilde{V}_{\text{p-h}}(q)$ from the static structure function $S(k)$ through the sum rules (16) and (17).

- ("xRPA") We have then added exchange effects to the equations of motion. In that case, we solve Eq. (10). The interactions in the "direct" and "exchange" channels, $\tilde{V}_{\rm dd}(q)$ and $\tilde{V}_{\rm ex}(q)$ respectively, are taken from FHNC calculations. The modification of the direct channel interaction is necessary in order to satisfy the sum rules (16) and (17) when exchanges are included. The dynamic response function no longer has the simple form (14).

- ("2p2h") Alternatively, we have added the energy-dependent corrections to the direct-channel interactions, *i.e.* used the direct channel interactions (18) and (19) and left out exchanges. This corresponds to our calculations of Refs. 1 and 9. The direct channel interaction is then $\widetilde{V}_{\text{p-h}}(q)$.

- ("x2p2h") Finally, we have added exchanges to the energy dependent interactions. The direct channel interactions, which are then given by Eqs. (18) and (19) but with $\widetilde{V}_{\text{p-h}}(q)$ replaced by $V_{\rm dd}(q)$.

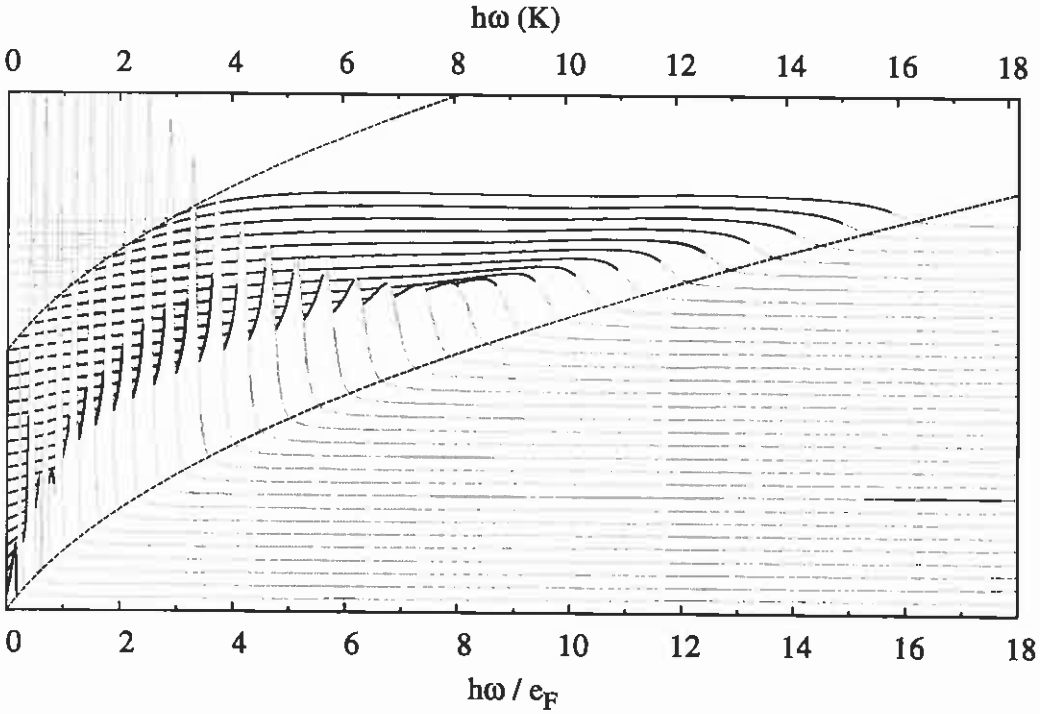

FIG. 4. The figure shows $S(q;\omega)$ for a sequence of wave numbers $k = 0.1k_F, \ldots k = 3.0k_F$ in steps of $\Delta k = 0.1k_F$ with increasing y-offset for the density $\rho = 0.02\,\text{Å}^{-2}$. The dashed lines indicate the boundaries of the $1p-1h$ continuum, outside of it the $S(q;\omega)$-curves are drawn in gray. Note that due to pair-fluctuations $S(q;\omega) \neq 0$ at the boundaries and therefore the dashed line coincides with the *projection* of the curve to its offset x-axis.

An overview of our results is shown in Figs. 4 - 6. In all of these calculations we have included both dynamic interactions and exchanges.

At all densities, we see the typical RPA picture of a collective mode, and a particle-hole continuum. At low densities, we do not see much of the "roton-like" excitation that was reported in Ref. 1. The mentioned feature appears very clearly at high densities.

A second effect that has not been observed in 3D ^{3}He is that the phonon is Landau damped at low densities. Landau damping occurs when the speed of sound is less that the Fermi velocity.

Taking the fit

$$E/N = A\rho + B\rho^2 + C\rho^3 \tag{29}$$

for the energy per particle at density ρ, with $A = 15.5227\,\text{KÅ}^2$, $B = -720.04\,\text{KÅ}^4$ and

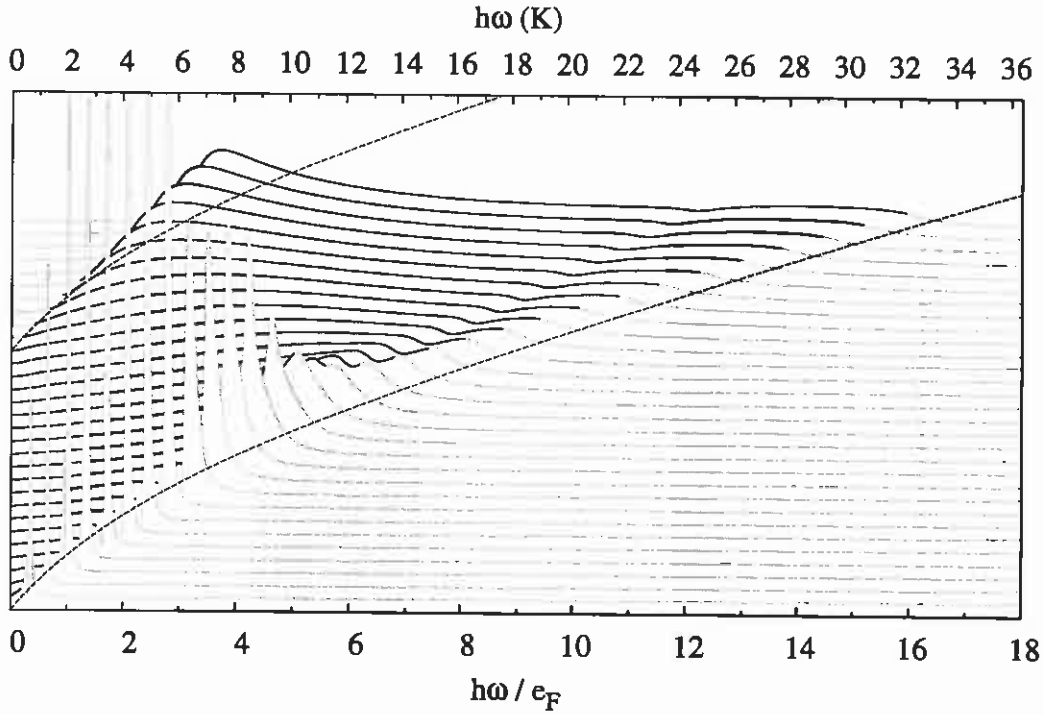

FIG. 5. Same as Fig. 4 for a density of $\rho = 0.04\,\text{Å}^{-2}$.

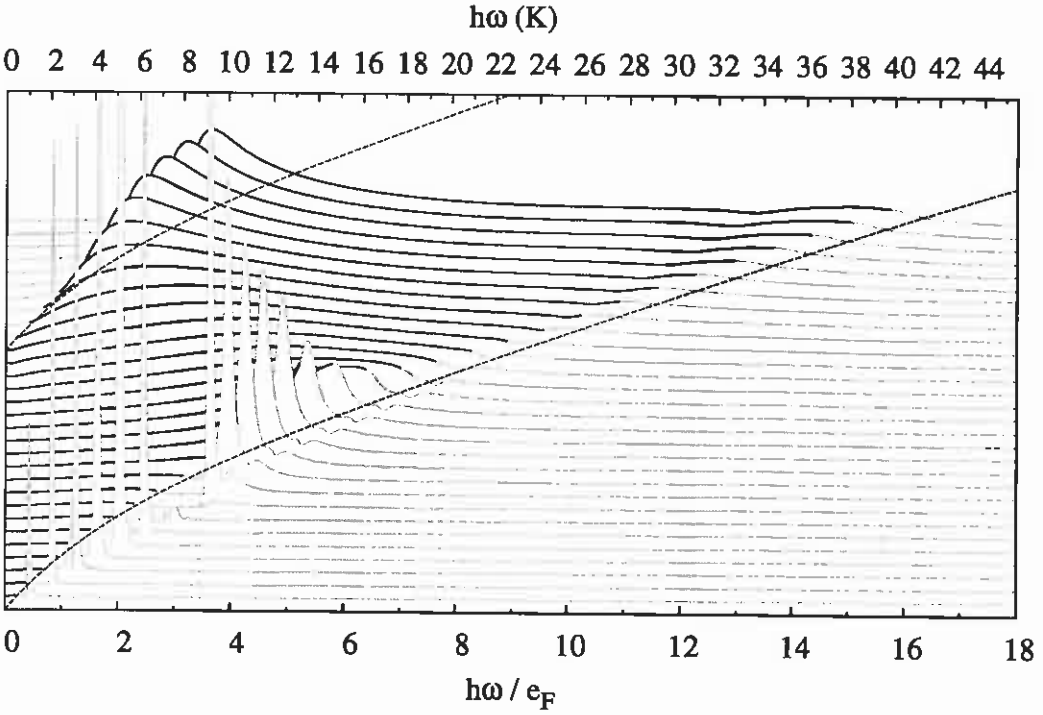

FIG. 6. Same as Fig. 4 for a density of $\rho = 0.05\,\text{Å}^{-2}$.

$C = 1.6953 \times 10^4\,\mathrm{K\AA}^6$ from Ref. 15 to calculate the hydrodynamic speed of sound, and comparing with the Fermi velocity $v_F = \hbar k_F/m$, one concludes that Landau damping occurs at densities below $\rho = 0.032\,\mathrm{\AA}^{-2}$. This agrees with our results. We note, however, that the Fermi velocity is lowered by an effective mass larger than 1. If a more realistic single particle spectrum[10] were used, the theory might indeed predict, at low densities and very long wave lengths, a stable collective excitation. The effective mass enhancement at the Fermi surface is, however, known to die out very quickly with energy. In the momentum regime where neutron scattering measurements can be done, the effective mass enhancement is not visible. Thus, a more detailed study of this momentum regime should await experimental progress.

From a theoretical point of view, it is of interest to determine the importance of individual physical effects. A major point of our previous work was that single-particle excitations and pair fluctuations do not have much to do with each other, and that the energy of the apparent "roton minimum" is unrelated to the location of the particle–hole band, but rather determined by fluctuations of the wave function at a scale of the inter-particle distance. This is quite plausible because the same effect, namely the lowering of the roton energy relative to the Feynman spectrum, is also observed in ^{4}He which does not have a particle–hole band yet strong pair fluctuations. Of course, if a "collective mode" merges with the particle-hole band it is strongly Landau damped.

Let us start with the discussion of the detailed results at the higher density $\rho = 0.04\,\mathrm{\AA}^{-2}$. The dynamic many-body correlations add, as a qualitatively new feature, a multipair continuum outside the particle-hole band. Adding an exchange term to the single particle spectrum (11) also modifies the boundaries of the particle-hole band as pointed out above; this modification should not be considered to be quantitative below perhaps $\hbar\omega \approx 0.5 e_F$.

Figs. 7 and 8 show $S(q;\omega)$ at selected long and short wave lengths for the four types of calculations outlined above. The particle-hole band extends, for $q \leq 2k_F$, down to zero energy. At wave numbers up to the Fermi wave number k_F, all calculations predict sharp collective modes. Outside the particle-hole band, the curves of RPA and xRPA have been artificially broadened to make them visible. It appears that xRPA pushes the collective mode to slightly larger energies. The dynamic theory also predicts collective modes outside the 1p-1h continuum. These modes are, however, naturally broadened by the 2p-2h background. As the momentum transfer increases, the effect of pair fluctuations lowers the energy of that collective excitation. Around $q = 1.5\,k_F$ we observe the transition of the collective excitation

into the 1p-1h band, the details depend on the specifics on the calculation and the position of the 1p-1h band.

The situation changes drastically around twice the Fermi wave number, see Fig. 8. The strengths predicted by both the RPA and the xRPA calculation are consistently at higher wave numbers than those obtained by the dynamic calculations. The latter predicts a rapid drop in the location of the maximum of $S(q;\omega)$ as a function of momentum transfer. Around $q \approx 2.5k_F$, the effect is enhanced by exchanges, whereas exchanges seem to push the strength again upwards at shorter wave lengths.

To assess the validity of these findings, we point out that he form of the pair propagator (20) still assumes a RPA-like spectrum of the intermediate states, this is most easily seen in the Bose limit. In a more self-consistent calculation, one should also add self-energy corrections to the pair propagator. We know from bosons that this lowers the spectrum and leads, among others, to the to the Pitaevskii-plateau[26], which would not have the right energy within the present implementation of our theory. A similar effect is expected for Fermions. The issue is, of course, a little speculative and basically means that our calculations lose reliability with at wave lengths significantly beyond the roton. On the other hand, higher-order fluctuations are known to lower the roton minimum in ^{4}He; the Bose limit of our theory brings the roton minimum of the Feynnman spectrum, which is at about 18 K, down to 11.7 K which still falls short of the experimental value of 8.7 K. To summarize, we expect that our method somewhat underestimates the downward shift of the roton that this underestimate becomes more severe with increasing wave number.

^{3}He in two dimensions is a gas, and therefore does not undergo a spinodal decomposition. This means that one can, in principle, carry out measurements at low densities. We have already discussed that one can expect, depending on the spectrum, Landau damping of the zero-sound mode at long wave lengths. In our case, the influence of exchange interactions is apparently so large that an effective collective mode can appear through shift of the particle-hole band. We note here that, at such long wave lengths, spin-fluctuations cause a further enhancement of the effective mass, hence a sharp collective mode should exist. On the other hand, pair fluctuations have practically no quantitative consequence. The observation persists throughout all wave vectors, see Fig. 9.

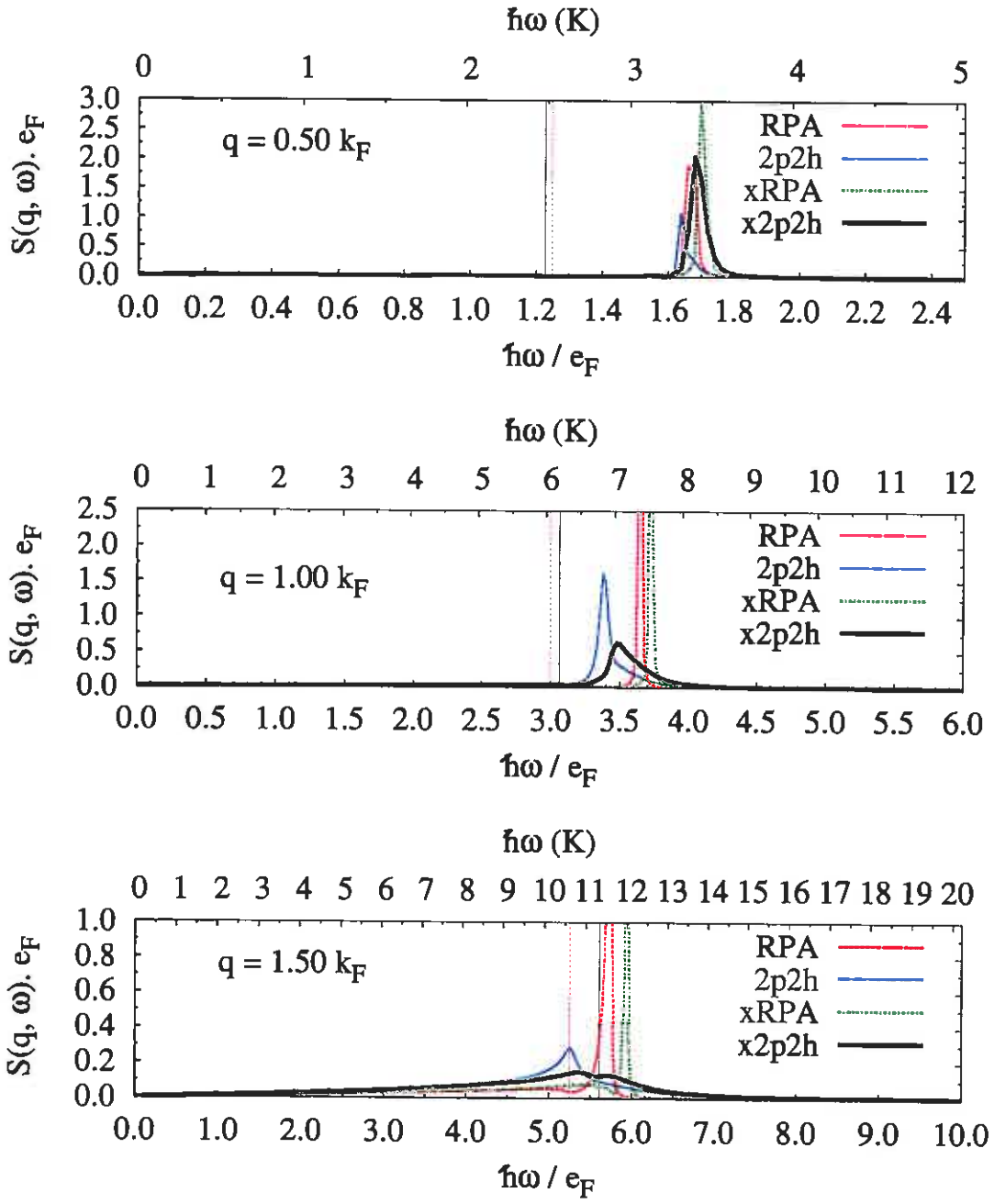

FIG. 7. (color online) The figure shows, for selected long wave lengths, a comparison of different calculations of $S(q;\omega)$ at a density of $\rho = 0.04\,\text{Å}^{-2}$. Shown are the four types of calculations "RPA", "xRPA", "'2p2h" and "2p2h" described above, and as marked in the figure. Also shown are the boundaries of the particle-hole band with and without exchanges (vertical lines, solid for xRPA and dashed for RPA). The RPA and xRPA results were artificially broadened, the (x)2p2h results have a natural width due to pair fluctuations.

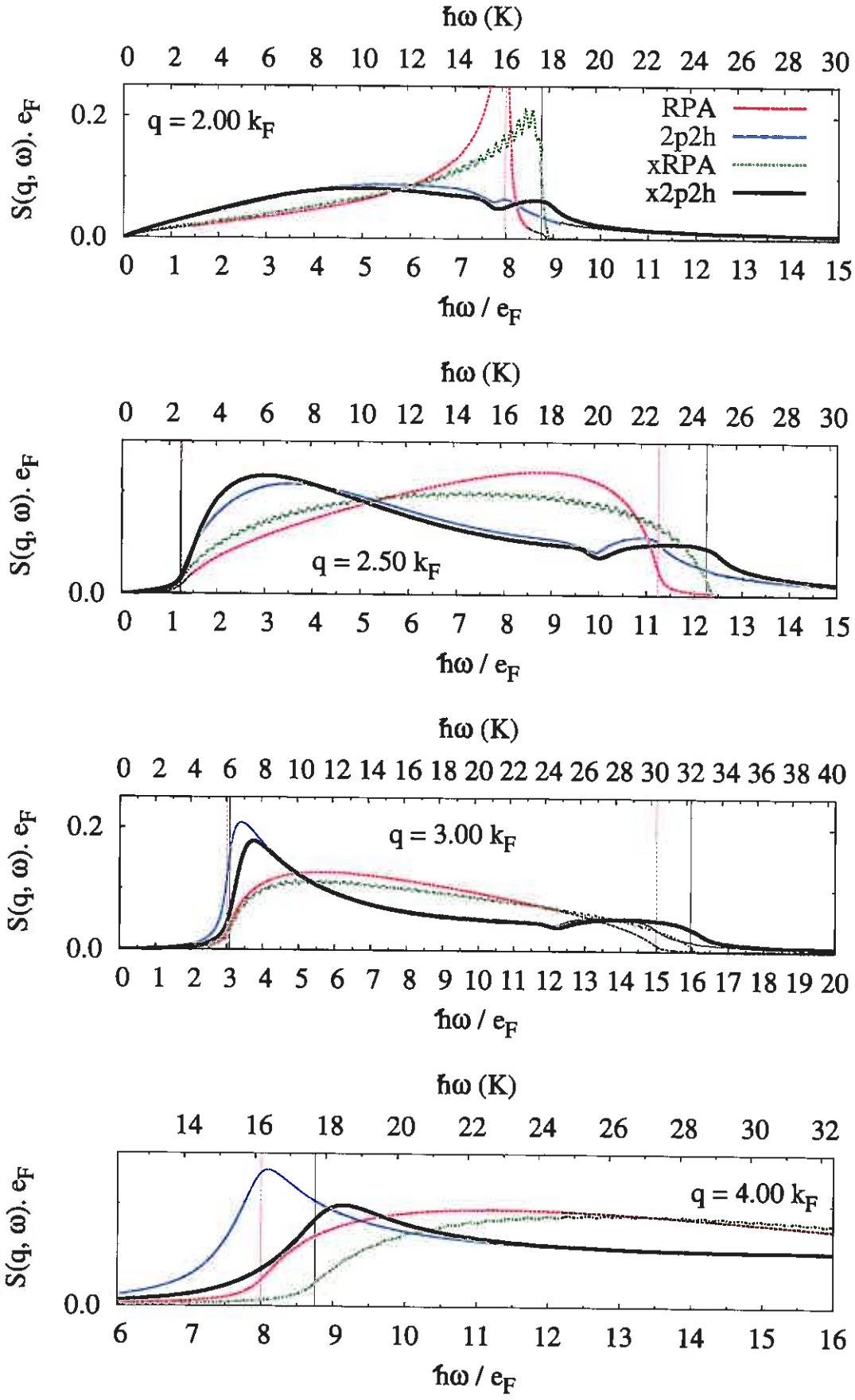

FIG. 8. (color online) Same as Fig. 7 for high wave numbers. The slight wiggles in the calculations containing exchange diagrams are numerical artifacts.

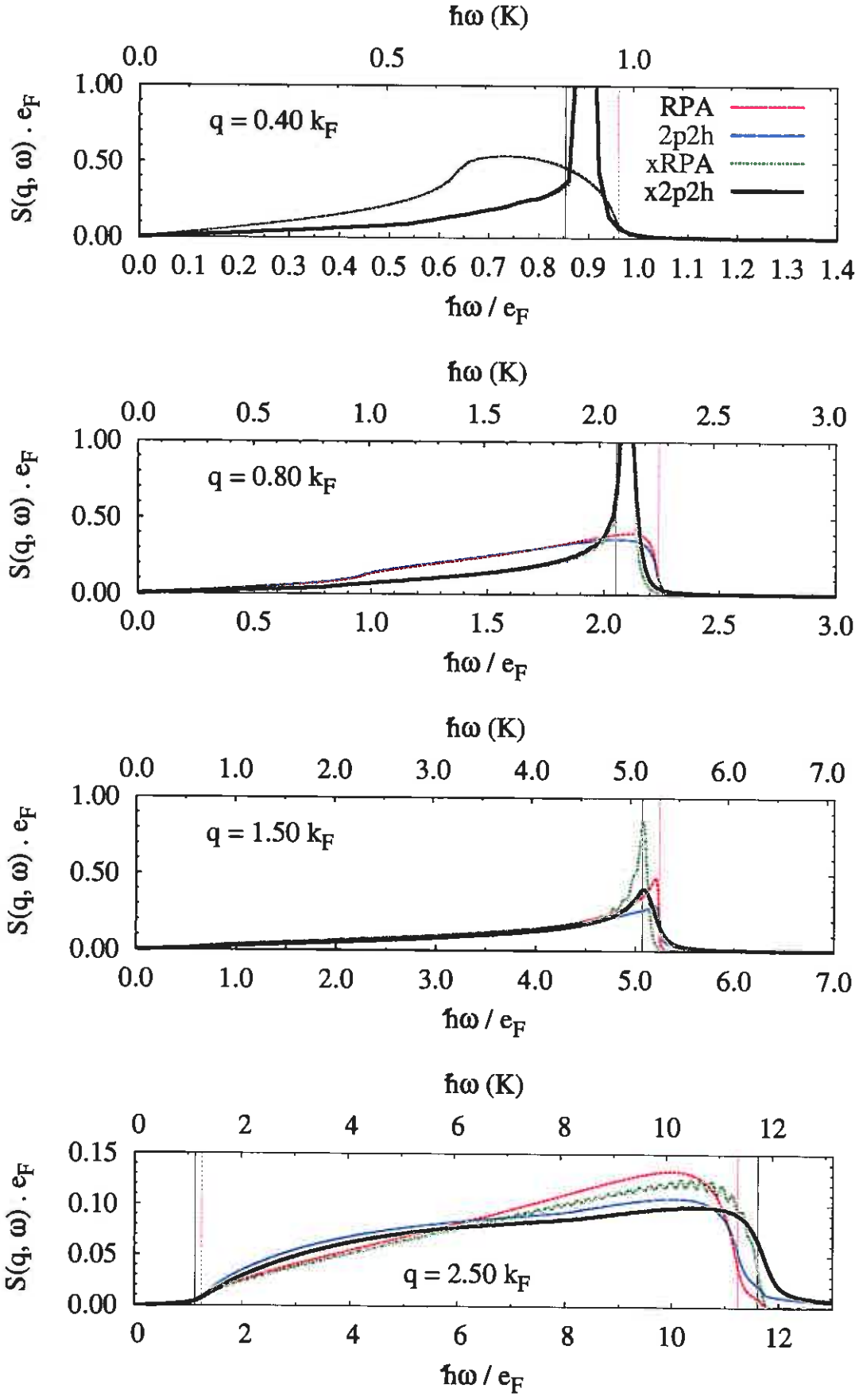

FIG. 9. (color online) Same as Fig. 7 for a density of $\rho = 0.02\,\text{Å}^{-2}$.

IV. SUMMARY

We have in this paper presented a study of the influence of exchange effects in the dynamic structure of two-dimensional ^{3}He. The essential findings have been mentioned in our discussion of the results. Let us reiterate here first the basic theoretical objectives of our work: The key to a quantitatively correct description of the dynamics of ^{3}He – and, therefore, other strongly correlated Fermi many-body systems – is the fact that, for excitations at atomic wave lengths, the *short-ranged* structure of the wave function is time dependent. The intermediate states can be described only in terms of the quantum numbers of at least two particles. With that strategy we have achieved a remarkably good agreement with experiments[1,9].

Evidently we are quite satisfied with the determination of ground state properties using the FHNC-EL scheme. In fact, from the comparison with FHNC-EL results[3] for ^{3}He in three dimensions, our results are better than expected.

In the description of the dynamics, we have included exchange as well as pair-excitations. We found that exchange effects may have some consequence for the dispersion of a potential collective mode at long wave lengths, in particular the possibility of a Landau-damped collective mode. Unfortunately, these momentum transfers are presently outside experimental reach. The most exciting aspect of our work, namely the appearance of a sharp mode at the edge or below the particle-hole continuum is hardly modified by the inclusion of exchanges.

There are two points where we see the potential of improvement: First, the influence of spin-fluctuations on the low-energy single-particle spectrum. The spectrum (11) is rather smooth and misses the strong peak in the effective mass around the Fermi wave number caused by spin-fluctuations. Hence, to make statements at these low energies, as they will be needed when measurements of the spin-structure function become available, the single particle spectrum (11) will have to be replaced by a dynamic self-energy.

The second point of improvement is the structure of the energy denominator. As discussed above, every correction towards a self-consistent picture should bring the energetics of the spectrum further down. The possibility to find the analog of a "Pitaevskii plateau" in either 2D or 3D ^{3}He makes this point a challenge for further work.

ACKNOWLEDGMENTS

This work was supported, in part, by the Austrian Science Fund FWF under grants P21264 and I602 (to EK) and by a study abroad fellowship through the Marshall plan to Robert Holler. Discussions with F. M. Gasparini are gratefully acknowledged. We also thank Jordi Boronat for providing unpublished data for the static structure function $S(k)$ shown in Fig. 2. We also thank A. Sultan and H. Godfrin for providing the experimental data shown in Fig. 2 prior to publication[17].

---

[1] H. Godfrin, M. Meschke, H.-J. Lauter, A. Sultan, H. M. Böhm, E. Krotscheck, and M. Panholzer, Nature **483**, 576579 (2012).

[2] H. R. Glyde, B. Fåk, N. H. van Dijk, H. Godfrin, K. Guckelsberger, and R. Scherm, Phys. Rev. B **61**, 1421 (2000).

[3] E. Krotscheck, J. Low Temp. Phys. **119**, 103 (2000).

[4] A. Fabrocini, S. Fantoni, and E. Krotscheck, *Introduction to Modern Methods of Quantum Many-Body Theory and their Applications*, Advances in Quantum Many–Body Theory, Vol. 7 (World Scientific, Singapore, 2002).

[5] H. M. Böhm, R. Holler, E. Krotscheck, and M. Panholzer, Phys. Rev. B **82**, 224505/1 (2010).

[6] H. W. Jackson, Phys. Rev. A **8**, 1529 (1973).

[7] E. Feenberg, *Theory of Quantum Fluids* (Academic, New York, 1969).

[8] C. C. Chang and C. E. Campbell, Phys. Rev. B **13**, 3779 (1976).

[9] E. Krotscheck and M. Panholzer, J. Low Temp. Phys. **163**, 1 (2011).

[10] J. Boronat, J. Casulleras, V. Grau, E. Krotscheck, and J. Springer, Phys. Rev. Lett. **91**, 085302 (2003).

[11] D. S. Greywall, Phys. Rev. B **41**, 1842 (1990).

[12] K.-D. Morhard, C. Bäuerle, J. Bossy, Y. Bunkov, S. N. Fisher, and H. Godfrin, Phys. Rev. B **53**, 2658 (1996).

[13] A. Casey, H. Patel, J. Nyéki, B. P. Cowan, and J. Saunders, Phys. Rev. Lett. **90**, 115301 (2003).

[14] V. Grau, J. Boronat, and J. Casulleras, Phys. Rev. Lett. **89**, 045301 (2002).

[15] J. Boronat, in *Microscopic Approaches to Quantum Liquids in Confined Geometries*, edited by

E. Krotscheck and J. Navarro (World Scientific, Singapore, 2002) pp. 21–90.

[16] J. Boronat(2002), private communication.

[17] A. Sultan, M. Meschke, H.-J. Lauter, and H. Godfrin(2012), this issue.

[18] P. Kramer and M. Saraceno, *Geometry of the time-dependent variational principle in quantum mechanics*, Lecture Notes in Physics, Vol. 140 (Springer, Berlin, Heidelberg, and New York, 1981).

[19] A. K. Kerman and S. E. Koonin, Ann. Phys. (NY) **100**, 332 (1976).

[20] D. J. Thouless, *The quantum mechanics of many-body systems*, 2nd ed. (Academic Press, New York, 1972).

[21] E. Krotscheck and J. W. Clark, Nucl. Phys. A **328**, 73 (1979).

[22] C. H. Aldrich and D. Pines, J. Low Temp. Phys. **25**, 677 (1976).

[23] H. W. Jackson, Phys. Rev. A **9**, 964 (1974).

[24] E. Krotscheck, Phys. Rev. A **26**, 3536 (1982).

[25] M. Panholzer, *Pair excitations and exchange effects in the dynamics of strongly correlated Fermifluids*, Ph.D. thesis, Johannes Kepler Universität Linz (2010).

[26] L. P. Pitaevskii, Zh. Eksp. Theor. Fiz. **36**, 1168 (1959), [Sov. Phys. JETP **9**, 830 (1959)].